PROCEEDINGS OF SCIENCE

CP-odd Higgs boson production in two-photon processes

Ken Sasaki
Dept. of Physics, Faculty of Engineering, Yokohama National University
Yokohama 240-8501, Japan
E-mail: sasaki@ynu.ac.jp

Tsuneo Uematsu*
Institute for Liberal Arts and Sciences, Kyoto University, Yoshida, Kyoto 606-8501, Japan
and Maskawa Institute, Kyoto Sangyo University, Kyoto 603-8555,Japan
E-mail: uematsu@scphys.kyoto-u.ac.jp

We discuss the CP-odd Higgs boson production through the two-photon processes in $e\gamma$ collisions. First we briefly review the Standard Model Higgs boson production in $e\gamma$ collisions, with special attention to transition form factor and differential production cross section. We then study the production of the CP-odd Higgs boson A^0 which appears in the extended Higgs sector such as the Minimal Supersymmetric Standard Model (MSSM) or in the Two-Higgs Doublet Models (2HDM). The electroweak one-loop contributions to the scattering amplitude for $e\gamma \to eA^0$ as well as the transition form factor are calculated and expressed in an analytical form. We found that one-loop contribution only comes from top-quark loops. There are no contributions from W-boson loop nor from stop loop. Numerical analysis for the production cross section is presented. It turns out that the $\gamma^*\gamma$-fusion is far more dominant over the $Z^*\gamma$-fusion.

13th International Symposium on Radiative Corrections (Applications of Quantum Field Theory to Phenomenology)
25-29 September, 2017
St. Gilgen, Austria

*Speaker.

PoS(RADCOR2017)066

1. Introduction

The Higgs boson with mass about 125 GeV was discovered by ATLAS and CMS at LHC [1] and its spin, parity and couplings were examined [2]. Now it would be intriguing to study its nature in e^+e^- collisions provided by such as linear collider [3]. Along with e^+e^- collider, other options such as e^-e^-, $e^-\gamma$ and $\gamma\gamma$ colliders have also been discussed. See Refs. [4]-[8] and the references therein. We first summarize what we have studied in [9, 10] about standard model (SM) Higgs boson H production through two-photon processes in $e\gamma$ collisions where the scattered electron detected in the final state (single tagging) shown in Fig.1. We calculated the so-

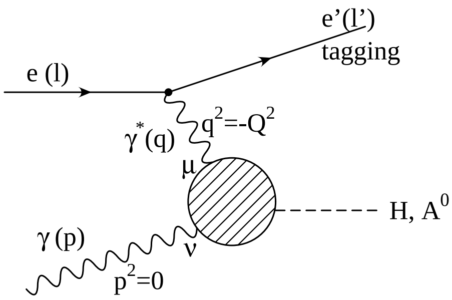

Figure 1: SM Higgs or CP-odd Higgs boson production in $e\gamma$ collision

called “transition form factor”as well as the production cross section, especially their Q^2 (virtual photon mass squared) dependence. It turned out at one-loop order the W-boson loop gives dominant contribution compared to the top-quark loop contribution.

We then extend our argument to CP-odd Higgs boson production in two-photon process of $e\gamma$ collisions [11]. In contrast to SM Higgs boson H, CP-odd Higgs A^0 has much simpler structure in transition form factor. We found that one-loop contribution only comes from top-quark loops. There are no contributions from W-boson loop nor from stop loop. Numerical analysis for the production cross section is presented. It turns out that the $\gamma^*\gamma$-fusion is far more dominant over the $Z^*\gamma$-fusion.

2. SM Higgs production in $e\gamma$ collision

The scattering amplitude for $e(l)+\gamma(p)\to e'(l')+H(q+p)$ shown in Fig.2 is given by

$$\langle e'H|T|e\gamma\rangle = \bar{u}(l')(-ie\gamma^\mu)u(l)\frac{-i}{q^2+i\varepsilon}A_{\mu\nu}\varepsilon^\nu(p) \tag{2.1}$$

where $\varepsilon^\nu(p)$ is the polarization vector of the incident real photon. Here we have introduced the tensor $A_{\mu\nu}$ which can be decomposed due to gauge invariance as

$$A_{\mu\nu}(q,p) = \left(g_{\mu\nu}(q\cdot p) - p_\mu q_\nu\right)S_1(m^2,Q^2,m_H^2) + \left(q_\mu p_\nu - \frac{q^2}{q\cdot p}p_\mu p_\nu\right)S_2(m^2,Q^2,m_H^2) \tag{2.2}$$

where $q^2=-Q^2<0$, $p^2=0$ and $(q+p)^2=p_H^2=m_H^2$. We denote collectively the mass of the intermediate particle in the loop by m. Since $p^\nu\varepsilon_\nu(p)=0$, only S_1 is relevant for the scattering

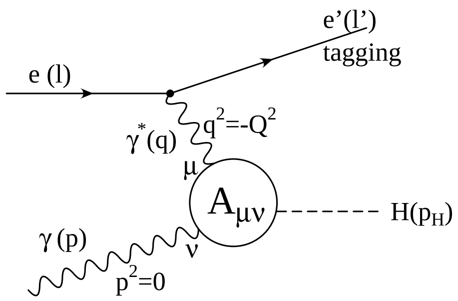

Figure 2: The transition amplitude for Higgs production via virtual and real photon fusion.

amplitude. We define the "transition form factor" $F_i(m^2, Q^2, m_H^2)$ by

$$F_i(m^2, Q^2, m_H^2) = S_1(m^2, Q^2, m_H^2) / \left(\frac{ge^2}{(4\pi)^2} \frac{1}{m_W} \right) \tag{2.3}$$

where $i = 1/2, 1$ for a fermion-loop $F_{1/2}$ and for the W-boson loop F_1, respectively. e and g are the electromagnetic and weak gauge couplings, respectively, and m_W is the W boson mass.

The total transition form factor is given by

$$F_{\text{total}}(Q^2, m_H^2) = \sum_f N_c e_f^2 F_{1/2}(m_f^2, Q^2, m_H^2) + F_1(m_W^2, Q^2, m_H^2) \tag{2.4}$$

where N_c is the number of the colors (1 for leptons and 3 for quarks) and e_f is the electric charge of the fermion f in the unit of proton charge. Evaluating the production cross section from Eq.(2.4), we found that at the one-loop level the W-loop contribution dominates over top-quark loop [9, 10].

3. MSSM/2HDM and A^0 production

We now consider a minimal extension of the Higgs sector of the Standard Model (SM). Here we investigate the Two-Higgs Doublet Model (2HDM) for the type-II case which includes the MSSM as a special case [12]. We denote the two SU(2)$_L$ doublets H_1,H_2, with weak hypercharge $Y = -1$ and $Y = 1$, respectively, by the 4 complex scalar fields, ϕ_1^0, ϕ_1^-, ϕ_2^+, ϕ_2^0 as follows:

$$H_1 = \begin{pmatrix} H_1^1 \\ H_1^2 \end{pmatrix} = \begin{pmatrix} \phi_1^{0*} \\ -\phi_1^- \end{pmatrix}, \quad H_2 = \begin{pmatrix} H_2^1 \\ H_2^2 \end{pmatrix} = \begin{pmatrix} \phi_2^+ \\ \phi_2^0 \end{pmatrix} \tag{3.1}$$

where, in the type II model, H_1 (H_2) only couples to the down-type (up-type) quarks and leptons. They acquire the following vacuum expectation values after the spontaneous symmetry breaking:

$$\langle H_1 \rangle = \begin{pmatrix} v_1 \\ 0 \end{pmatrix}, \quad \langle H_1 \rangle = \begin{pmatrix} 0 \\ v_2 \end{pmatrix}, \quad \tan\beta = v_2/v_1 \tag{3.2}$$

Then 3 degrees of freedom out of 8 consisting of the 4 complex scalar fields are absorbed by the longitudinal components of $W^\pm$, Z, and the remaining 5 physical degrees of freedom become the following two charged and three neutral physical Higgs bosons:

$$\text{Charged} \quad H^+, H^-; \quad \text{CP-even} \quad h^0, H^0; \quad \text{CP-odd} \quad A^0 \tag{3.3}$$

Here we are particularly interested in the CP-odd Higgs boson A^0, and investigate its transition form factor and the production cross section in the $\gamma^*\gamma$-fusion process.

We now enumerate some characteristics of the coupling of A^0 for the type II case:

1) In contrast to the CP-even Higgs bosons h^0 and H^0, A^0 does not couple to W^+W^- and ZZ pairs at tree level. Hence W-boson and Z-boson one-loop diagrams do not contribute to the A^0 production.

2) A^0 does not couple to other two physical Higgs bosons in cubic interactions.

3) The couplings of A^0 to the fermions are proportional to the fermion masses. Therefore, we only consider the top quark for the charged fermion loop diagrams. The A^0 coupling to the top quark with mass m_t is given by $\lambda\gamma_5$ with [12]

$$\lambda = -\frac{g m_t \cot\beta}{2m_W} \ . \tag{3.4}$$

Here g and m_W are the weak gauge coupling and the weak boson mass, respectively.

4) In the case of MSSM, the trilinear A^0 coupling to mass-eigenstate squark pairs $\tilde{q}_i\tilde{q}_i$ $(i=1,2)$ vanishes [12]. Hence, the scalar top-quark (stop) does not contribute to the A^0 production in $e\gamma$ collisions at one-loop level.

3.1 Scattering Amplitude for $\gamma^*\gamma$ Fusion Process

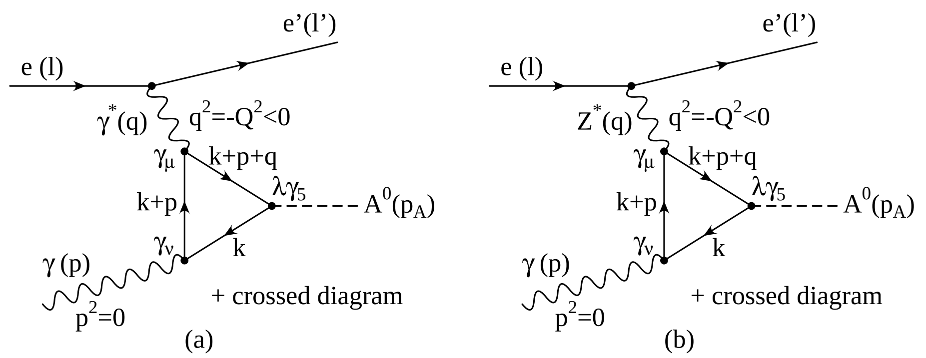

Figure 3: (a) $\gamma^*\gamma$ fusion diagram for $e\gamma \to e'A^0$ (b) $Z^*\gamma$ fusion diagram for $e\gamma \to e'A^0$

We first consider the case of $\gamma^*\gamma$ fusion process as shown in Fig.3(a). Since p is the momentum of a real photon, we have $p^2=0$ and $p^\nu\varepsilon_\nu(p)=0$, where $\varepsilon_\nu(p)$ is the photon polarization vector. We set virtual photon momentum $q=l-l'$. Assuming that electrons are massless so that $l^2={l'}^2=0$, we introduce the following Mandelstam variables:

$$q+p=p_A, \quad q^2=-Q^2, \quad p^2=0 \tag{3.5}$$

$$s \ = \ (l+p)^2 = 2l\cdot p\ , \quad t=(l-l')^2=q^2=-Q^2=-2l\cdot l', \tag{3.6}$$

$$u \ = \ (p-l')^2 = -2l'\cdot p = m_A^2 - s - t\ . \tag{3.7}$$

where $p_A^2 = m_A^2$ with m_A being the CP-odd Higgs boson mass.

We evaluate the top-loop amplitude for the $\gamma^*\gamma$ fusion diagram as shown in Fig.3(a):

The scattering amplitude for $e(l) + \gamma(p) \to e'(l') + A^0(p_A)$ is given by

$$\langle e'A|T|e\gamma\rangle_{\gamma^*\gamma} = \overline{u}_{r'}(l')(-ie\gamma_\mu)u_r(l)\frac{-i}{q^2+i\varepsilon}A^{\mu\nu}\varepsilon_\nu(p,\lambda_2) \tag{3.8}$$

where $\varepsilon_\nu(p,\lambda_2)$ is the polarization vector of the incident real photon with momentum p and helicity λ_2. The $u_r(l)$ ($\overline{u}_{r'}(l')$)is the spinor for the initial (scattered) electron with momentum l (l') and helicity r (r'). The tensor $A_{\mu\nu}$ is given as

$$A_{\mu\nu} = -8ie^2 m_t \lambda \varepsilon_{\mu\nu\alpha\beta} q^\alpha p^\beta \int \frac{d^4k}{(2\pi)^4} \frac{1}{[k^2-m_t^2][(k+p)^2-m_t^2][(k+p+q)^2-m_t^2]} \; . \tag{3.9}$$

3.2 One-loop integrals

The above one-loop integral (3.9) is given by the three-point scalar integral by Passarino-Veltman [13]:

$$\frac{1}{(2\pi)^4}\int d^4k \frac{1}{[k^2-m_1^2][(k+p_2)^2-m_2^2][(k+p_1+p_2)^2-m_3^2]} = \frac{i\pi^2}{(2\pi)^4}C_0(p_1^2,p_2^2,p_3^2,m_1^2,m_2^2,m_3^2) \tag{3.10}$$

In our present case of e and real γ collision we have

$$C_0(-Q^2,0,m_A^2,m_t^2,m_t^2,m_t^2) = -\frac{1}{Q^2+m_A^2}\left\{\frac{1}{2}g(\rho)+2f(\tau)\right\} \tag{3.11}$$

where the dimesionless variables τ and ρ are defined as

$$\tau \equiv \frac{4m_t^2}{m_A^2}, \quad \rho \equiv \frac{Q^2}{4m_t^2} \tag{3.12}$$

and the two functions $f(\tau)$ and $g(\rho)$ we have introduced are given by

$$f(\tau) = \left[\sin^{-1}\sqrt{\frac{1}{\tau}}\right]^2 \qquad \tau \geq 1 \tag{3.13}$$

$$= -\frac{1}{4}\left[\log\frac{1+\sqrt{1-\tau}}{1-\sqrt{1-\tau}} - i\pi\right]^2 \qquad \tau < 1 \tag{3.14}$$

$$g(\rho) = \left[\log\frac{\sqrt{\rho+1}+\sqrt{\rho}}{\sqrt{\rho+1}-\sqrt{\rho}}\right]^2 \tag{3.15}$$

Thus we have [11]

$$A_{\mu\nu} = \frac{ge^2}{(4\pi)^2}\frac{\cot\beta}{2m_W}\frac{\tau}{1+\rho\tau}[g(\rho)+4f(\tau)]\;\varepsilon_{\mu\nu\alpha\beta}q^\alpha p^\beta \tag{3.16}$$

where we have used the relation $\lambda = -gm_t\cot\beta/2m_W$. Similar combinations of functions $f(\tau)$ and $g(\rho)$ as in Eq.(3.11) with the time-like virtual mass, appear in the Higgs decay processes $H \to \gamma^*\gamma$ and $H \to Z^*\gamma$ in Ref.[14] (see also Ref.[12] for on-shell decays, $H \to \gamma\gamma$ [15] and $H \to Z\gamma$).

3.3 Transition Form Factor

We can define the so-called "Transition Form Factor" as in the case of the standard Higgs boson. Now first we note

$$A_{\mu\nu}(q,p) \equiv \tilde{S}(m_t^2, Q^2, m_A^2)\varepsilon_{\mu\nu\alpha\beta}q^\alpha p^\beta \tag{3.17}$$

where we now introduce the transition form factor $\tilde{F}$ as

$$\begin{aligned}\tilde{F}(m_t^2, Q^2, m_A^2) &\equiv \tilde{S}_1(m_t^2, Q^2, m_A^2)/\left(\frac{ge^2}{(4\pi)^2}\frac{1}{m_W}\right) \\ &= -\frac{1}{2}\frac{\tau}{1+\rho\tau}[g(\rho)+4f(\tau)] = 4m_t^2 C_0 \end{aligned} \tag{3.18}$$

Since $\tau = (2m_t/m_A)^2$ we have the following two cases depending on the mass of A^0.

For $m_A < 2m_t$ *i.e.* $\tau > 1$ we have $f(\tau)$ given by Eq.(3.13) which is a real function. While for $m_A > 2m_t$ *i.e.* $\tau < 1$ we have $f(\tau)$ given by Eq.(3.14) which is a complex function. Therefore, the former is real while the latter becomes complex.

We also introduce the total transition form factor $\tilde{F}_{\text{total}}$ which includes the all the flavors of the quark-loop, but dominated by top loop.

$$\tilde{F}_{\text{total}}(Q^2) = \sum_f N_c q_f^2 \tilde{F}(\rho_f, \tau_f) \simeq 3\cdot\left(\frac{2}{3}\right)^2 \tilde{F}(m_t^2, Q^2, m_A^2) \tag{3.19}$$

We consider the two cases: (a) $m_A = 300$ GeV and (b) $m_A = 400$ GeV shown below (Fig.4(a),(b)).

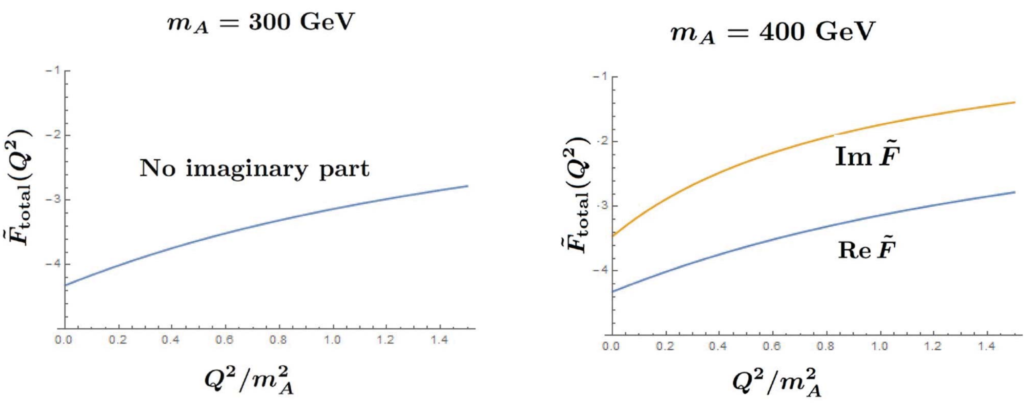

(a) (b)

Figure 4: Transition Form Factor for the mass (a) $m_A = 300$GeV (b) $m_A = 400$GeV

3.4 Differential cross section

The differential cross section for the CP-odd Higgs production via $\gamma^*\gamma$ fusion in $e\gamma \to eA^0$ is given by

$$\frac{d\sigma(\gamma^*\gamma)}{dQ^2} = \frac{\alpha_{\rm em}^3}{64\pi}\frac{g^2}{4\pi}\frac{1}{Q^2}\left[1+\frac{u^2}{s^2}\right]\frac{1}{m_W^2}|\tilde{F}_{\rm total}(Q^2)|^2 \tag{3.20}$$

where $\alpha_{\rm em} = e^2/4\pi$. Since $s = 2l\cdot p$ and $u = -2p\cdot l'$ we note $u = m_A^2 + Q^2 - s$. Hence we obtain

$$\frac{d\sigma(\gamma^*\gamma)}{dQ^2}\Big/\frac{\alpha_{\rm em}^3}{64\pi}\frac{g^2}{4\pi} = \frac{1}{Q^2}\left[1+\frac{(m_A^2+Q^2-s)^2}{s^2}\right]\frac{1}{m_W^2}\left|\frac{4}{3}\tilde{F}(m_t^2, Q^2, m_A^2)\right|^2 \tag{3.21}$$

3.5 Z boson and real γ fusion

The scattering amplitude for $e(l)+\gamma(p) \to e'(l')+A^0(p_A)$ via $Z^*\gamma$ fusion shown in Fig.3(b) is

$$\langle e'A|T|e\gamma\rangle_{Z^*\gamma} = \frac{g}{4\cos\theta_W}\overline{u}_{r'}(l')(i\gamma_\mu)(f_{Ze}+\gamma_5)u_r(l)\frac{-i}{q^2-m_Z^2}\widetilde{A}^{\mu\nu}\varepsilon_\nu(p,\lambda_2) \tag{3.22}$$

where

$$\widetilde{A}_{\mu\nu} = 8e\frac{g}{4\cos\theta_W}m_t\lambda f_{Zt}\frac{1}{16\pi^2}C_0(-Q^2,0,m_A^2,m_t^2,m_t^2,m_t^2)\varepsilon_{\mu\nu\alpha\beta}q^\alpha p^\beta \tag{3.23}$$

and e-e-Z coupling f_{Ze} and t-t-Z coupling f_{Zt} are given by

$$f_{Ze} = (-1+4\sin^2\theta_W), \qquad f_{Zt} = (1-\frac{8}{3}\sin^2\theta_W). \tag{3.24}$$

Note that the scattering amplitudes both from $\gamma^*\gamma$-fusion and $Z^*\gamma$-fuison should be added up. When taking absolute square of the amplitude we get an interference term, which turns out to be positive, in addition to the $\gamma^*\gamma$- as well as $Z^*\gamma$- fusion terms as follows:

$$\frac{d\sigma}{dQ^2}(\text{total}) = \frac{d\sigma}{dQ^2}(\gamma^*\gamma-\text{fusion})+\frac{d\sigma}{dQ^2}(Z^*\gamma-\text{fusion})+\frac{d\sigma}{dQ^2}(\text{Interference}) \tag{3.25}$$

4. Numerical Analysis

4.1 production cross section

First let us note that the contribution from the $\gamma^*\gamma$ fusion is far more dominant over that from $Z^*\gamma$-fusion as well as the interference term. We have shown the differential cross sections for the three process in Fig.5 in the case of $\sqrt{s} = 500$GeV, $m_t = 173$GeV, $m_A = 400$GeV, $\cot\beta = 1$. (In fact, the cross sections are proportional to $\cot^2\beta$.) We observe that at $Q^2 = 1000$ (5000) GeV^2 the ratio of $d\sigma/dQ^2(Z^*\gamma)$ to $d\sigma/dQ^2(\gamma^*\gamma)$ is 4.3×10^{-6} (5.2×10^{-5}) and $d\sigma/dQ^2$(Interference) to $d\sigma/dQ^2(\gamma^*\gamma)$ is 4.1×10^{-3} (1.4×10^{-2}). Thus the Z^*-boson exchange reaction does not actually affect the $\gamma^*\gamma$ exchange process (Fig.3). This means that the transition form factor makes sense for the A^0 production in $e\gamma$ collision.

Now we shall focus on the $\gamma^*\gamma$ fusion process based on the formula for the production cross section Eq.(3.20). In Fig.6 we have plotted the differential production cross section of A^0 with

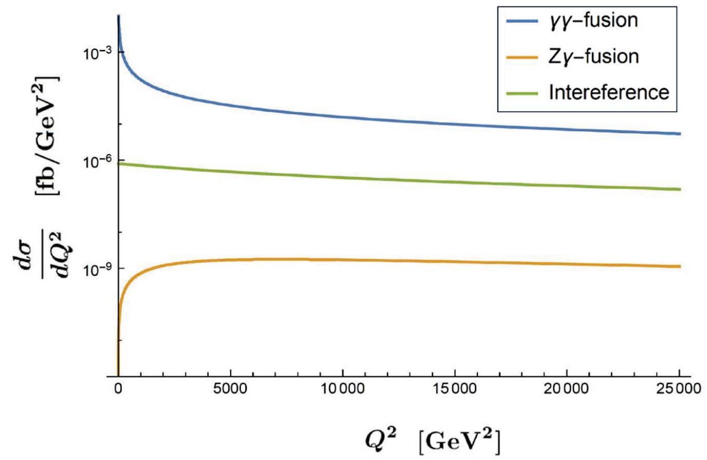

Figure 5: Comparison of the contributions from 3 processes:$\gamma^*\gamma$-fusion, $Z^*\gamma$-fusion and Interference for $\sqrt{s} = 500$GeV, $m_t = 173$GeV, $\cot\beta = 1$, $m_A = 400$GeV.

mass $m_A = 200,\ 300,\ 400$ GeV, for $\sqrt{s} = 500$ GeV and $m_t = 173$ GeV. We find that for this kinematical region the production cross section for A^0 increases as m_A gets larger which looks somewhat unexpected result.

We can examine this behaviour in more detail by computing the differential cross section for fixed Q^2, which we take to $(100)^2$ GeV^2.

4.2 The A^0 mass dependence of the production cross section

We have plotted the A^0 mass dependence of the differential cross section $d\sigma/dQ^2$ for $Q^2 = (100)^2$ GeV^2 in Fig.7(a) as well as that for the total cross section σ_{total} in Fig.7(b). As m_A varies across the $t\bar{t}$ threshold $2m_t \approx 346$GeV, the differential cross section $d\sigma/dQ^2$ increases in the region $m_A < 2m_t$, and it turns to decrease when m_A goes beyond $2m_t$.

In both cases, we see the strong kink structure corresponding to the threshold effect at $m_A = 2m_t \approx 346$ GeV.

5. Conclusion

In this talk we have investigated the possible production of the CP-odd Higgs boson A^0 which would appear in the 2HDM/MSSM through $e\gamma$ collisions. In contrast to the SM Higgs boson H as well as to the CP-even Higgs boson h^0 and H^0, the A^0 does not couple to W^+W^- and ZZ pairs because of the CP-odd nature. Hence at one-loop order $W^\pm$ bosons do not contribute to triangle diagrams for the A^0 production, and only top-quark one-loop triangle diagram is relevant. There is no scalar top-quark (stop) contribution. The transition form factor shows much simpler structure.

When the mass of the A^0 boson, m_A is smaller than $2m_t$ the transition form factor is a real function of Q^2, while if m_A is larger than $2m_t$, the transition form factor becomes complex. The

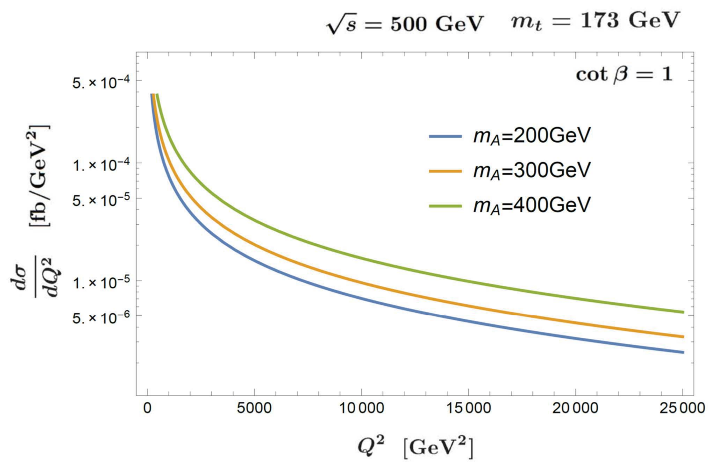

Figure 6: Differential cross section for the production of CP-odd Higgs boson A^0 with mass $m_A = 200,\ 300,\ 400$ GeV.

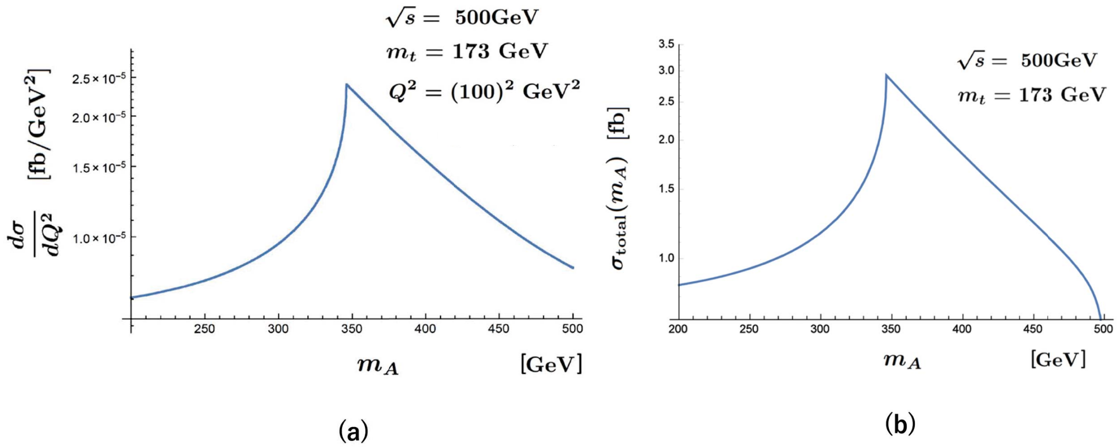

Figure 7: (a) The A^0 mass dependence of the differential cross section for the CP-odd Higgs production with $Q^2 = (100)^2\mathrm{GeV}^2$ (b) The A^0 mass dependence of the total cross section for the CP-odd Higgs production.

production cross section of CP-odd Higgs boson is given by the absolute square of the transition form factor together with some kinematical factors.

For a fixed value of m_A, the differential production cross section shows a decreasing function of Q^2. On the other hand, if we fix Q^2 and vary the mass of A^0, it increases as m_A for $m_A < 2m_t$ and decreases for $m_A > 2m_t$. This feature is common with the total cross section.

In the $e\gamma$ scattering, the contribution from the $\gamma^*\gamma$ fusion is far more dominant over that from $Z^*\gamma$ fusion. Thus actually we only have to consider the photon- exchange diagram, and it makes sense to talk about the transition form factor of A^0.

Acknowledgments

We would like to thank the organizers of the RADCOR 2017 for the hospitality at such a well-organized and stimulating symposium.

References

[1] ATLAS Collaboration, *Phys. Lett.* **B716**, 1 (2012); CMS Collaboration, *Phys. Lett.* **B716**, 30 (2012).

[2] ATLAS Collaboration, *Phys. Lett.* **B726**, 88 (2013); *Phys. Lett.* **B726**, 120 (2013); CMS Collaboration, *Phys. Rev. Lett.* **110**, 081803 (2013).

[3] http://www.linearcollider.org.

[4] A. De Roeck, "Physics at a $\gamma^*\gamma$, $e\gamma$ and e^-e^- Option for a Linear Collider", arXiv:hep-ph/0311138 (2003).

[5] V. I. Telnov, *Nucl. Instrum. Meth.* **A455**, 63 (2000) [hep-ex/0001029]; B. Badelek *et al.*, *Int. J. Mod. Phys.* **A19**, 5097 (2004) [hep-ex/0108012]; M. M. Velasco *et al.*, *eConf* **C010630**, E3005 (2001) [hep-ex/0111055].

[6] M. Melles, W. J. Stirling and V. A. Khoze, *Phys. Rev.* **D61**, 054015 (2000); M. Melles, *Nucl. Phys. Proc. Suppl.* **82**, 379 (2000); G. Jikia and S. Soldner-Rembold, *Nucl. Phys. Proc. Suppl.* **82**, 373 (2000); M. M. Mühlleitner, M. Krämer, M. Spira and P. M. Zerwas, Phys. Lett. **B508** (2001) 311; M. M. Mühlleitner, *Acta Phys. Polon.* **B37** 1127 (2006), [hep-ph/0512232]; D. M. Asner, J. B. Gronberg, and J. F. Gunion, *Phys. Rev.* **D67**, 035009 (2003); S. J. Brodsky, *Int. J. Mod. Phys.* **A20**, 7306 (2005); P. Niezurawski, *eConf* **C050318**, 0503 (2005).

[7] S. A. Bogacz et al., "SAPPHiRE: a Small $\gamma\gamma$ Higgs Factory", arXiv:1208.2827 [physics.acc-ph] (2012).

[8] I. F. Ginzburg and M. Krawczyk, "Testing Higgs Physics at the Photon Collider", arXiv:1310.5881 [hep-ph] (2013); I. F. Ginzburg and M. V. Vychugin, *Physics of Atomic Nuclei*, **67**, (2004) 281.

[9] N. Watanabe, Y. Kurihara, K. Sasaki and T. Uematsu, *Phys. Lett.* **B728**, 202 (2014); PoS (RADCOR 2013) 050; PoS (RADCOR 2013) 053; PoS (QFTHEP 2013) 040.

[10] N. Watanabe, Y. Kurihara, T. Uematsu,and K. Sasaki, *Phys. Rev.* **D90**, 033015 (2014).

[11] K. Sasaki and T. Uematsu, arXiv:1712.00197 [hep-ph] (2017).

[12] J. F. Gunion, H. E. Haber, G. Kane and S. Dawason, "The Higgs Hunter's Guide"(Addison-Wesley, 1990).

[13] G. Passarino and M. Veltman, *Nucl. Phys.* **B160**, 151 (1979); G. 't Hooft and M.J.G. Veltman, *Nucl. Phys.* **B153**, 365 (1979); G.J. van Oldenborgh and J.A.M. Vermaseren, *Z. Physik* **C46** 425 (1990).

[14] J.C. Romao and S. Andringa, *Eur. Phys. J. C.* **7**, 631 (1997).

[15] J. Ellis, M. K. Gaillard and D. V. Nanopoulos, *Nucl. Phys.* **B106**, 292 (1976); B. L. Ioffe and V. A. Khoze, *Sov. J. Part. Nucl.* **9**, 50 (1978); M. A. Shifman, A. I. Vainshtein, M. B. Voloshin and V. I. Zakharov, *Sov. J. Nucl. Phys.* **30**, 711 (1979); *Phys. ReV.* **D85**, 013015 (2012); T. G. Rizzo, *Phys. ReV.* **D22**, (1980) 178; M. B. Gavela, G. Girardi, C. Malleville and P. Sorba, *Nucl. Phys.* **B193**,257 (1981); W. J. Marciano, C. Zhang and S. Willenbrock, *Phys. ReV.* **D85**, 013002 (2012).